^{11}C-Labeled KF18446: A Potential Central Nervous System Adenosine A_{2a} Receptor Ligand

Kiichi Ishiwata, Junko Noguchi, Shin-ichi Wakabayashi, Junichi Shimada, Nobuo Ogi, Tadashi Nariai, Akira Tanaka, Kazutoyo Endo, Fumio Suzuki, and Michio Senda

Positron Medical Center, Tokyo Metropolitan Institute of Gerontology, Tokyo; Showa College of Pharmaceutical Sciences, Tokyo; Department of Neurosurgery, Tokyo Medical and Dental University, Tokyo; and Pharmaceutical Research Laboratories, Kyowa Hakko Kogyo Company, Shizuoka, Japan

To develop PET ligands for mapping central nervous system (CNS) adenosine A_{2a} receptors that are localized in the striatum and are coupled with dopamine receptors, 3 ^{11}C-labeled xanthine-type adenosine A_{2a} antagonists, [^{11}C]KF18446 ([7-methyl-^{11}C]-(*E*)-8-(3,4,5-trimethoxystyryl)-1,3,7-trimethylxanthine), [^{11}C]KF19631 ([7-methyl-^{11}C]-(*E*)-1,3-diallyl-7-methyl-8-(3,4,5-trimethoxystyryl-)xanthine), and [^{11}C]CSC ([7-methyl-^{11}C]-8-chlorostyrylcaffeine), were compared with [^{11}C]KF17837 ([7-methyl-^{11}C]-(*E*)-8-(3,4-dimethoxystyryl)-1,3-dipropyl-7-methylxanthine). **Methods:** The regional brain uptake of the tracers, the effect of the coinjected adenosine antagonists on the uptake, and the metabolism were studied in mice. In rats, the regional brain uptake of the tracers was visualized by ex vivo autoradiography (ARG). The A_{2a} receptor binding of antagonist 1 was also measured by in vitro ARG. Imaging of the monkey brain was performed with PET with antagonist 1. **Results:** In mice, the highest striatal uptake was found for antagonist 1 followed by antagonists 2 and 4. The uptake was inhibited by each of 3 KF compounds and by CSC, but not by an A_1 antagonist KF15372. Another selective nonxanthine-type A_{2a} antagonist SCH 58261 significantly decreased the striatal uptake of only antagonist 1, the labeled metabolites of which were less than 20% in the plasma 30 min postinjection, but were negligible in the brain tissue. In ex vivo ARG, antagonist 1 showed the highest striatal uptake and the highest uptake ratio of the striatum to the other brain regions. A high and selective binding of antagonist 1 to the striatum was also confirmed by in vitro ARG. PET with antagonist 1 visualized adenosine A_{2a} receptors in the monkey striatum. **Conclusion:** These results indicate that antagonist 1 ([^{11}C]KF18446) is the most suitable PET ligand for mapping adenosine A_{2a} receptors in the CNS.

Key Words: ^{11}C-KF18446; adenosine A_{2a} receptor; striatum; central nervous system; PET

J Nucl Med 2000; 41:345–354

Adenosine is an endogenous modulator of several physiological functions in the central nervous system (CNS) as well as in peripheral organs. The effect is mediated by 2 major subtypes of receptors: adenosine A_1 receptors, which exhibit a higher affinity to adenosine and inhibit adenylyl cyclase; and A_2 receptors, which exhibit a lower affinity to adenosine and stimulate adenylyl cyclase. Recent advances in molecular biology and pharmacology have demonstrated the presence of at least 4 subtypes: A_1, A_{2a}, A_{2b}, and A_3 receptors (*1–3*).

In the CNS, adenosine A_1 receptors are present both pre- and postsynaptically in many regions, being abundant in the hippocampus, cerebral cortex, thalamic nuclei, basal ganglia, and the cerebellar cortex in animals (*4–6*) and humans (*7*). On presynaptic terminals, their main action is to limit the availability of calcium to the excitation-secretion coupling mechanism involved in the exocytotic release of neurotransmitters such as glutamate, acetylcholine, dopamine, 5-hydroxytryptamine, and several peptides (*8*). Postsynaptically, adenosine A_1 receptors usually induce hyperpolarization of cells, at least partly by opening potassium channels (*8*).

Adenosine A_{2a} receptors are highly concentrated in the striatum, nucleus accumbens, and olfactory tubercle, in which dopamine D_1 and D_2 receptors are localized with very high densities, whereas A_{2b} receptors show a ubiquitous distribution (*9,10*). Recent studies also demonstrated the presence of A_{2a} receptors in the hippocampus and cortex (*11–14*). The A_{2a} receptors have been reported to induce effects opposite to those of A_1 receptors. By the in situ hybridization technique, adenosine A_{2a} receptor mRNA and dopamine D_2 receptor mRNA are found to be mainly expressed in striatopallidal γ-aminobutyric acid (GABA)-ergic–enkephaline neurons (*15,16*). In patients with Huntington's chorea with selective degeneration of the striatopallidal neurons, the adenosine A_{2a} receptor density is significantly reduced in the striatum, whereas the density is not significantly affected in patients with Parkinson's disease, characterized by selective degeneration of nigrostriatal dopamine neurons (*17*). One of the most potentially important actions of adenosine relevant to motor control is that of modulating dopamine receptors. Activation of adenosine A_{2a} receptors reduced the affinity of dopamine D_2 receptors for agonist ligands (*18*). The selective adenosine A_{2a} receptor agonist CGS 21680 was found to reduce apomorphine-induced turning (*19*). On the other hand, it is known that a typical neuroleptic haloperidol increased the density of adenosine

Received May 27, 1998; revision accepted Jun. 22, 1999.

For correspondence or reprints contact: Kiichi Ishiwata, PhD, Positron Medical Center, Tokyo Metropolitan Institute of Gerontology, 1-1 Naka-cho, Itabashi-ku, Tokyo 173-0022, Japan.

A_{2a} receptors in the rat striatum (*20*). Thus, recent pharmacological and biochemical data suggest the presence of a receptor-receptor interaction between adenosine A_{2a} and dopamine D_2 receptors in the striatum (*21,22*).

Adenosine receptors in central and peripheral nervous systems have been considered as targets for new drugs in many neurological diseases (*8,22–24*). In treating patients with Parkinson's disease, L-dopa is not effective for approximately 40% of the patients, and its use over several years may lead to loss of efficacy. Adenosine therapy offers promise as an alternative or adjunct therapy (*8*). In treating schizophrenia with neuroleptics, chronic administration of haloperidol or fluphenazine frequently results in the development of severe movement disorders (*25*). Animal experiments suggest that adenosine A_{2a} receptors are associated with antipsychotic activity of the neuroleptics through interaction with dopamine receptors (*26*). The various therapeutic possibilities of agonists or antagonists of adenosine receptors in neurological and psychiatric disorders have been reviewed (*22–24*).

Based on this background, PET assessment of the adenosine receptor system probably offers a new diagnostic tool for neurological disorders as well as an opportunity to understand the neurotransmission system more completely from the viewpoint of neuroscience. Therefore, we have developed PET ligands for the 2 adenosine receptor subtypes: [^{11}C]KF15372 ([3-propyl-^{11}C]-8-dicyclopropylmethyl-1,3-dipropylxanthine) (*27*) and its methyl and ethyl derivatives (*28*) for adenosine A_1 receptors, and [^{11}C]KF17837 ([7-methyl-^{11}C]-(*E*)-8-(3,4-dimethoxystyryl)-1,3-dipropyl-7-methylxanthine) for the adenosine A_{2a} receptors (*29,30*). In previous studies (*27*), the selectivity of [^{11}C]KF15372 and its derivatives as PET adenosine A_1 receptor ligands have been demonstrated, and the decreased A_1 receptor density in the superior colliculus was detected by ex vivo autoradiography (ARG) in rats deprived of retinocollicular fibers by contralateral eye enucleation. As an adenosine A_{2a} receptor ligand, [^{11}C]KF17837, which has a high affinity for the A_{2a} receptors, was preferentially taken up by the striatum in mice, rats, and monkeys (*30*) and was also taken up to a smaller extent by the cortex and cerebellum. In rodents, the uptake of [^{11}C]KF17837 was shown to be A_{2a}-receptor mediated, because the striatal uptake was blocked by adenosine A_{2a} receptor antagonists but not by an A_1 receptor antagonist. A similar blocking effect was also observed in the cortex and cerebellum, suggesting that the selectivity of [^{11}C]KF17837 for the adenosine A_{2a} receptors may not be sufficient as a PET tracer. Furthermore, Stone-Elander et al. (*31*) did not detect with PET any significant blocking effect of unlabeled KF17837 on the striatal uptake of [^{11}C]KF17837 in monkeys measured, probably because of low signal-to-noise ratio as a result of low penetration of the [^{11}C]KF17837 into the blood–brain barrier and low administered dose. Therefore, we decided to find a more selective PET ligand for mapping the adenosine A_{2a} receptors in the CNS.

In this study, we prepared 3 other xanthine-type adenosine A_{2a} receptor antagonists: [^{11}C]KF18446 ([7-methyl-^{11}C]-(*E*)-8-(3,4,5-trimethoxystyryl)-1,3,7-trimethylxanthine), [^{11}C]KF19631 ([7-methyl-^{11}C]-(*E*)-1,3-diallyl-7-methyl-8-(3,4,5-trimethoxystyryl)xanthine), and [^{11}C]CSC ([7-methyl-^{11}C]-8-chlorostyrylcaffeine, [7-methyl-^{11}C]-8-chlorostyryl-1,3,7-trimethylxanthine), and compared them with [^{11}C]KF17837. Chemical structures of the 4 ^{11}C-labeled tracers are shown in Figure 1. KF18446 and KF19631 are new adenosine A_{2a} antagonists. CSC is currently used in pharmacological studies as a selective adenosine A_{2a} antagonist, but its affinity for the A_{2a} receptors (K_i, 54 nmol/L) (*32*) is lower than that of KF17837 (K_i, 1.0 nmol/L) (*33*). Among the 4 tracers the most selective candidate as a PET ligand is [^{11}C]KF18446.

MATERIALS AND METHODS

KF17837, KF18446, KF19631, CSC, and their desmethyl compounds, a nonxanthine adenosine A_{2a} antagonist 5-amino-7-(2-phenylethyl)-2-(2-furyl)pyrazolo[4,3-*e*]-1,2,4-triazolo[1,5-*c*]pyridine (SCH 58261), and an adenosine A_1 antagonist KF15372 were prepared by Kyowa Hakko Kogyo Company (Shizuoka, Japan). 2-[*p*-(2-carboxyethyl)phenethylamino]-5′-*N*-ethylcarboxamidoadenosine (CGS 21680) was purchased from Research Biochemical, Inc. (Natick, MA) and [^{3}H]CGS 21680 and N^6-[^{3}H]cyclohexyladenosine were obtained from New England Nuclear (Boston, MA).

Male ddY mice (7–9-wk-old) were obtained from Tokyo Laboratory Animals Company (Tokyo, Japan). Young male Wistar rats (8–9-wk-old) were supplied by the Animal Laboratory of the Tokyo Metropolitan Institute of Gerontology.

The animal studies were approved by the Animal Care and Use Committee of the Tokyo Metropolitan Institute of Gerontology.

Radiosynthesis

[^{11}C]KF17837, [^{11}C]KF18446, [^{11}C]KF19631, and [^{11}C]CSC were prepared by ^{11}C-methylation of the respective desmethyl compounds with [^{11}C]methyl iodide by the method previously described, with modifications for high-performance liquid chromatography (HPLC) separation (*29*). [^{11}C]Methyl iodide was trapped in 0.25 mL *N,N*-dimethylformamide containing 0.5 mg 7-desmethyl compound and 5 mg Cs_2CO_3. The solution was heated at

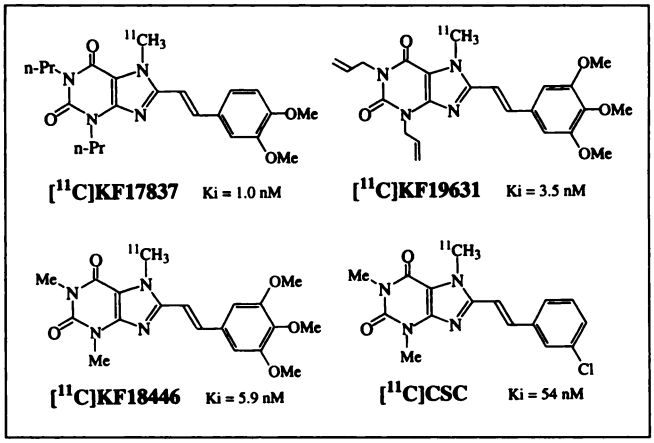

FIGURE 1. Chemical structures of 4 ^{11}C-labeled xanthine-type adenosine A_{2a} antagonists.

120°C for 1–5 min. After adding 1.25 mL 0.05 mol/L HCl, the reaction mixture was loaded onto an octyldecyl saline column (10-mm inside diameter/250 mm). The mobile phase was a mixture of acetonitrile and water at a flow rate of 10 mL/min. The ratios of acetonitrile to water (v/v) of the mobile phase and the retention times were 80/20 and 4.8 min for [^{11}C]KF17837, 60/40 and 5.5 min for [^{11}C]KF19631, 60/40 and 6.0 min for [^{11}C]CSC, and 60/40 and 3.0 min for [^{11}C]KF18446, respectively. The ^{11}C-labeled ligand fraction was collected and evaporated to dryness. The residue was dissolved in physiological saline containing 0.25% (v/v) Tween 80. The radiochemical purity of each of the ^{11}C-labeled ligands was >99%, which was determined by HPLC analysis as described (*30*). The final product included no starting materials. The radiochemical yields of 4 tracers were 25%–46%, and the specific radioactivity was 10–72 GBq/μmol at 20–25 min from the end of irradiation. All procedures were performed under dim light to prevent isomerization of the compounds (*29*).

In Vitro Affinity for Adenosine A_{2a} Receptors

In vitro affinity of KF18446 and KF19631 for adenosine A_{2a} and A_1 receptors was determined using the rat striatal membrane and [^{3}H]CGS 21680 as a radioligand and the rat forebrain membrane and N^6-[^{3}H]cyclohexyladenosine, respectively, as described (*33*). The affinity of other antagonists was available in the literature (Table 1).

Biodistribution in Mice

Each ^{11}C-labeled tracer (0.54–1.3 MBq/14–72 pmol) was intravenously injected into male ddY mice (33–41 g). They were killed by cervical dislocation at 5, 15, 30, and 60 min postinjection. The blood was collected by heart puncture, and the tissues were harvested and weighed. The ^{11}C in the samples was counted with an auto-γ-counter. The tissue uptake of ^{11}C was expressed as the percentage injected dose per gram tissue (%ID/g).

Regional Brain Distribution Study in Mice

The ^{11}C-labeled tracer was intravenously injected into male ddY mice. They were killed by cervical dislocation at 5, 15, 30, and 60 min postinjection. The brain was removed and divided into the striatum, cerebellum, cortex, and remaining tissue. The tissue uptake of radioactivity was measured as the %ID/g.

In another group, the tracer was coinjected together with 1 of 6 compounds: 4 xanthine-type adenosine A_{2a} antagonists, KF17837, KF18446, KF19631, and CSC; a nonxanthine-type adenosine A_{2a} antagonist SCH 58261 (*34*); and an A_1 antagonist KF15372 (*35*). The regional brain distribution of the radioactivity was measured at 15 min after injection. The amount of the coinjected antagonists was 50 nmol/animal for KF17837 and 100 nmol/animal for the others.

In a third group, [^{11}C]KF18446 with a different amount of carrier KF18446 was injected. The regional brain distribution of the radioactivity was measured at 15 min postinjection.

Metabolite Study

Mice were intravenously injected with [^{11}C]KF18446 (10–11 MBq/0.59–0.68 nmol) and killed by cervical dislocation at 5, 15, and 30 min postinjection (n = 3–4). All procedures described next were performed under dim light to prevent photoisomerization of [^{11}C]KF18446 (*29*). Blood was obtained by heart puncture using a heparinized syringe and was centrifuged to obtain plasma. The plasma was denatured with a third volume of 20% trichloroacetic acid in acetonitrile. The mixture was centrifuged at 7000*g* for 2 min. The precipitate was resuspended in 0.5 mL of 10% trichloroacetic acid in acetonitrile, followed by centrifugation. The treatment was repeated once. The striatum or cortex was homogenized in 0.5 mL of 10% trichloroacetic acid in acetonitrile. The homogenate was centrifuged at 7000*g* for 2 min, and the precipitate was treated as described earlier. Over 98% of radioactivity was recovered in the combined supernatant fractions. The supernatant for plasma, striatum, or cortex was diluted with water to make it 40% as acetonitrile. The sample of 0.5–1 mL was loaded onto a Nova-Pak C_{18} column equipped in an RCM 8 × 10 module (8 × 100 mm; Millipore-Waters, Milford, MA). The mobile phase was a mixture of acetonitrile and 50 mmol/L sodium acetate (pH 4.5; 4/6, v/v) at a flow rate of 2 mL/min. The elution profile was detected with a radioactivity monitor (FLO-ONE/β A-200; Radiomatic

TABLE 1
Effects of Coinjected Adenosine Antagonists on Regional Brain Distribution of Radioactivity at 15 Minutes After Intravenous Injection of 3 ^{11}C-Labeled Tracers into Mice

	%ID/g tissue			
Antagonist*	Blood	Cortex	Striatum	Cerebellum
[^{11}C]KF18446				
Control (23)	1.41 ± 0.35	1.55 ± 0.25	4.39 ± 0.97	1.62 ± 0.24
KF17837	1.50 ± 0.27	0.97 ± 0.05†	1.23 ± 0.30†	1.01 ± 0.10†
KF19631	1.38 ± 0.30	1.11 ± 0.12†	1.52 ± 0.15†	1.13 ± 0.15†
KF18446	1.63 ± 0.27	1.42 ± 0.07‡	1.55 ± 0.16†	1.50 ± 0.13
CSC (8)	1.63 ± 0.10	1.51 ± 0.10	3.04 ± 0.50†	1.35 ± 0.13†
SCH58261 (9)	1.51 ± 0.24	1.54 ± 0.12	2.10 ± 0.25†	1.81 ± 0.15
KF15372	1.21 ± 0.12	1.59 ± 0.09	4.12 ± 0.66	1.62 ± 0.08
[^{11}C]KF19631				
Control (15)	0.61 ± 0.09	1.27 ± 0.19	1.51 ± 0.19	1.55 ± 0.25
KF17837	1.63 ± 0.10	0.70 ± 0.09†	1.04 ± 0.44‡	0.83 ± 0.13†
KF19631	2.04 ± 0.18	0.75 ± 0.06†	1.09 ± 0.19†	0.89 ± 0.04†
KF18446	1.27 ± 0.22	1.21 ± 0.32	1.76 ± 0.36	1.49 ± 0.47
CSC (9)	1.66 ± 0.23	0.88 ± 0.14†	1.37 ± 0.32	0.99 ± 0.19†
SCH58261 (8)	0.67 ± 0.08	1.73 ± 0.27	2.02 ± 0.53	2.16 ± 0.36
KF15372	0.55 ± 0.05	1.43 ± 0.16	1.66 ± 0.39	1.71 ± 0.15
[^{11}C]KF17837§				
Control (28)	0.86 ± 0.13	1.68 ± 0.20	2.30 ± 0.43	1.97 ± 0.29
KF17837	1.19 ± 0.05	1.14 ± 0.02†	1.32 ± 0.09†	1.10 ± 0.03†
KF19631	1.54 ± 0.27	1.26 ± 0.12†	1.52 ± 0.42†	1.32 ± 0.24†
KF18446	1.34 ± 0.15	1.40 ± 0.15	1.73 ± 0.22†	1.55 ± 0.14†
CSC	1.16 ± 0.18	1.27 ± 0.26‖	2.02 ± 0.51	1.38 ± 0.29†
SCH 58261	1.07 ± 0.08	2.45 ± 0.39	2.75 ± 0.24	2.77 ± 0.55
KF15372	1.06 ± 0.09	1.83 ± 0.17	2.31 ± 0.37	2.07 ± 0.32

*Amounts of coinjected antagonists were 100 nmol/animal, except for 50 nmol/animal for KF17837.

†$P < 0.001$.

‡$P < 0.05$ (*t* test, compared to control).

§Part of data was also presented in reference 30.

‖$P < 0.01$.

K_i values for the adenosine A_{2a} and A_1 receptors are: 5.9 nmol/L and 1600 nmol/L for KF18446, 3.5 nmol/L and >10,000 nmol/L for KF19631, 1.0 nmol/L and 62 nmol/L for KF17837, 54 nmol/L and 28,000 nmol/L for CSC, 2.3 nmol/L and 121 nmol/L for SCH 58261, and 430 nmol/L and 3.0 nmol/L for KF15372. Mean ± SD (n = 4, unless indicated in the parenthesis). Injected doses: 0.8–1.3 MBq/~33–72 pmol/L.

Instruments & Chemical Company Inc., Tampa, FL). The radioactivity was recovered quantitatively. The retention time of [^{11}C]KF18446 was 6.2 min.

Ex Vivo ARG Study in Rats

Male Wistar rats (8–9-wk-old) were killed 15 min after intravenous injection of each of the 4 ^{11}C-labeled tracers (0.34–1.0 MBq/4.1–65 nmol/kg). The effect of coinjected carrier KF17837 (700 nmol/animal, approximately 2.8 μmol/kg) on the brain uptake of [^{11}C]KF18446 was also measured at 15 min postinjection. Coronal and sagittal brain sections were prepared as described previously (*27,28,30*). Regional brain uptake was analyzed using an imaging plate and a bioimaging analyzer of type BAS 3000 (FUJIX; Fuji Photo Film Co., Tokyo, Japan). The regional brain uptake of radioactivity was represented as the photostimulated luminescence (PSL), and expressed as the PSL/mm^2/MBq, in which the injected dose was decay-corrected at the contact time.

In Vitro ARG Study of [^{11}C]KF18446 in the Rat Brain Section

In vitro ARG was performed according to the method of Przedborski et al. (*36*). Coronal brain sections 20 μm thick were prepared from young male Wistar rats. The brain sections were preincubated in 50 mmol/L Tris–HCl, pH 7.4, containing 10 mmol/L $MgCl_2$ and 0.2 IU/mL adenosine deaminase for 30 min at room temperature. Then, the sections were incubated in the same buffer containing 2.3 nmol/L (100 kBq/mL) [^{11}C]KF18446 with and without 20 μmol/L cold KF18446 for 30 min at room temperature. Blocking effect of 20 μmol/L SCH 58261 or CGS 21680 on the [^{11}C]KF18446-binding was also examined. After being washed with ice-cold 50 mmol/L Tris–HCl, pH 7.4, containing 10 mmol/L $MgCl_2$, the brain sections were dried on a hot plate at 60°C and then apposed on the imaging plate. The tracer binding was measured as described earlier.

PET Study in a Monkey

A female rhesus monkey (22-y-old, 5.0 kg) was anesthetized with 0.01%–0.05% isoflurane, and PET scanning was performed as described previously (*30*). [^{11}C]KF18446 (102 MBq/2.2 nmol) was injected intravenously into the monkey, and time-sequential tomographic scanning was performed in the transverse section of the brain parallel to the orbitomeatal line for 60 min (10 frames for 1 min, 4 frames for 5 min, and 3 frames for 10 min). The PET camera was a model SHR 2000 (Hamamatsu Photonics, Hamamatsu, Japan). The camera consists of 4 ring detectors and acquires 7 slices at a center-to-center interval of 6.5 mm with a resolution of 4.0 mm full width at half maximum in the transaxial plane. Based on MRI images as described below, regions of interest (ROIs) were placed on the striatum, cortex, cerebellum, and thalamus, and the time–activity curve in the ROI was obtained for each scan of the brain as described (*30*). The decay-corrected radioactivity value was expressed as the standardized uptake value (SUV), (([regional activity/milliliter volume])/injected activity/gram body weight).

Blood was collected from a vein at 1, 5, 15, 30, and 60 min after the tracer injection, and after centrifugation the plasma was obtained. The radioactivity level of the plasma was assessed as the SUV, and the labeled metabolites were analyzed as previously described.

For MRI, the monkey, anesthetized with isoflurane, was positioned prone, and MRI was performed in the T2-weighted sequence (echo time/repetition time = 2000/80) parallel to the orbitomeatal line on a 4.7-T experimental imager/spectrometer system (Unity plus SIS 200/330; Varian, Palo Alto, CA). The slice thickness was 3 mm.

RESULTS

In Vitro Affinity for Adenosine A_{2a} Receptors

The K_i values of KF18446 were 5.9 nmol/L for the adenosine A_{2a} receptors and 1600 nmol/L for the adenosine A_1 receptors, and those of KF19631 were 3.5 nmol/L for the A_{2a} receptors and >10,000 nmol/L for the A_1 receptors. The affinity of the 2 compounds for the A_{2a} receptors was in the same magnitude of order as KF17837 (K_i, 1.0 nmol/L for the A_{2a} receptors and 62 nmol/L for the A_1 receptors) (*33*), and was approximately 10-fold higher than that of CSC (K_i, 54 nmol/L for the A_{2a} receptors and 28,000 nmol/L for the A_1 receptors) (*32*). Thus, the highest in vitro A_{2a}/A_1 selectivity was found for KF19631 (>2800), followed by [^{11}C]CSC (520), [^{11}C]KF18446 (270), and [^{11}C]KF17837 (62).

Biodistribution in Mice

Figure 2 shows the radioactivity levels (%ID/g) in the brain, plasma, heart, and kidney after injection of [^{11}C]KF18446, [^{11}C]KF19631, [^{11}C]CSC, or [^{11}C]KF17837 into mice. [^{11}C]CSC showed the highest brain uptake at 5 min after injection, followed by [^{11}C]KF18446, [^{11}C]KF19631, and [^{11}C]KF17837. However, the radioactivity of [^{11}C]CSC was rapidly washed out, whereas that of [^{11}C]KF18446 decreased more slowly and that of [^{11}C]KF19631 remained constant. The time course of [^{11}C]KF18446 and [^{11}C]KF19631 in the other tissues was similar to that of [^{11}C]KF17837 (*29*). The distribution pattern of [^{11}C]CSC was slightly different from that of the 3 KF compounds. The uptake of [^{11}C]CSC was relatively high in the lung and small intestine, and the radioactivity levels in all examined tissues decreased rapidly.

Regional Brain Distribution Study in Mice

Figure 3 summarizes the regional brain uptake of the 3 ^{11}C-labeled KF compounds in mice. The striatal uptake of [^{11}C]KF18446 was greater than that of [^{11}C]KF19631 or [^{11}C]KF17837. The uptake of [^{11}C]KF18446 gradually decreased with time, whereas that of [^{11}C]KF19631 increased. The uptake of [^{11}C]KF17837 increased until 30 min and then decreased. In the cortex and cerebellum, the uptake of [^{11}C]KF19631 also increased until 30 min and then decreased, whereas that of [^{11}C]KF18446 and [^{11}C]KF17837 gradually decreased. [^{11}C]KF18446 showed the highest uptake ratios of striatum-to-cortex and striatum-to-cerebellum. The ratios increased for the first 15–30 min, and then slightly decreased at 60 min. The uptake ratios for [^{11}C]KF19631 and [^{11}C]KF17837 increased with time.

To characterize the binding sites of 3 ^{11}C-labeled KF compounds, the blocking effects of the adenosine receptor antagonists on the regional brain uptake of the tracers were examined (Table 1). Each of the 4 xanthine A_{2a} antagonists reduced the striatal uptake of [^{11}C]KF18446 and [^{11}C]KF17837. The order of the blocking effect (KF17837 > KF19631 > KF18446 > CSC) paralleled their in vitro

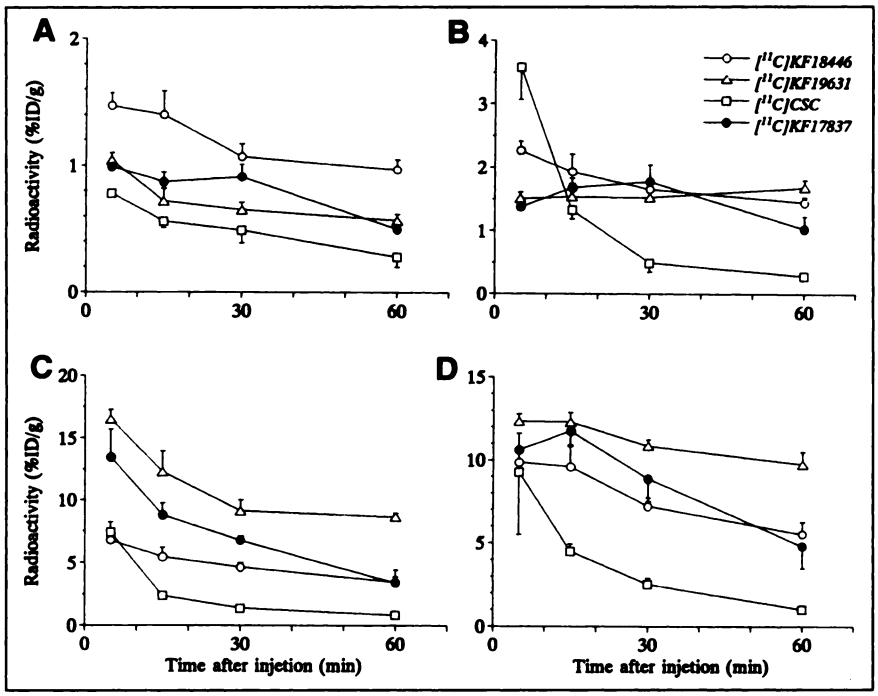

FIGURE 2. Time course of tissue radioactivity for blood (A), brain (B), heart (C), and kidney (D) after intravenous injection of [^{11}C]KF18446, [^{11}C]KF19631, [^{11}C]CSC, or [^{11}C]KF17837 into mice.

affinity. In the case of the striatal uptake of [^{11}C]KF19631, the blocking by KF18446 was not significant. A nonxanthine adenosine A_{2a} antagonist, SCH 58261 (K_i, 2.3 nmol/L for the A_{2a} receptors and 121 nmol/L for the A_1 receptors) (*34*) significantly decreased the striatal uptake of only [^{11}C]KF18446. The uptake of 3 tracers in the cortex and cerebellum was also slightly decreased with the coinjection of xanthine antagonists, but some of them did not have a significant effect. On the other hand, an adenosine A_1 antagonist KF15372 (K_i, 3.0 nmol/L for the A_1 receptors and 430 nmol/L for the A_{2a} receptors) (*35*) did not block the uptake of the 3 tracers in any regions.

Figure 4 shows the effect of carrier dose on the regional brain uptake of [^{11}C]KF18446. The striatal uptake remained high up to 0.3 nmol of the injected dose (~8.5 nmol/kg), and gradually decreased with increasing dose. The uptake by the cortex was significantly decreased to 78%–92% at the dose of 3 nmol and more. The significant reduction in the cerebellum was found only at 30 nmol. At the highest dose (100 nmol/animal, 2.9 μmol/kg), the uptake levels were comparable among the 3 regions.

Metabolite Study in Mice

In the HPLC analysis of plasma, in addition to [^{11}C]KF18446 (retention time of 6.2 min), unidentified labeled metabolites 1 and 2 were found at the retention times of 1.7 and 3.8 min, respectively. Percentage of unchanged [^{11}C]KF18446 in the plasma gradually decreased: 86.0 ± 3.5 (n = 3) at 5 min, 83.0 ± 5.3 (n = 3) at 15 min, and 80.8 ± 7.3 (n = 4) at 30 min. In the striatum and cortex, >98% of radioactivity was detected as the unchanged form over 30 min. Only a negligible amount of metabolite 2 was detected at 15 and 30 min.

Ex Vivo ARG Study in Rats

Figures 5A–D show the ex vivo autoradiographic images of the rat brain at 15 min postinjection. In the sagittal and

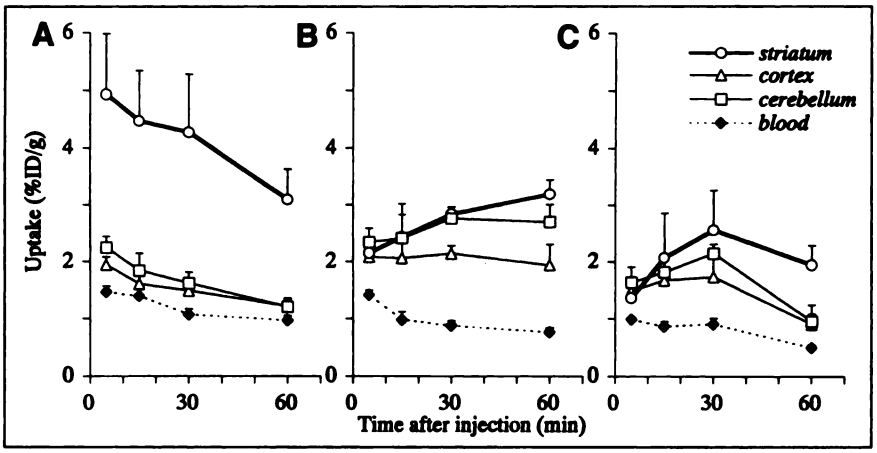

FIGURE 3. Regional brain distribution of radioactivity after intravenous injection of [^{11}C]KF18446 (A), [^{11}C]KF19631 (B), or [^{11}C]KF17837 (C) into mice.

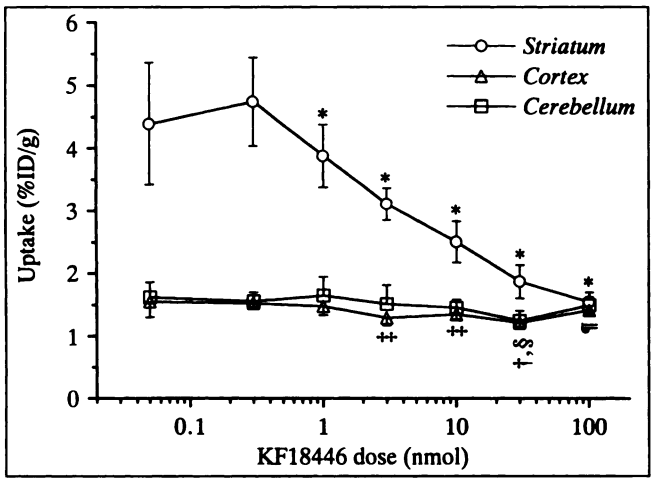

FIGURE 4. Effect of carrier dose on regional brain uptake of [^{11}C]KF18446 15 min after intravenous injection in mice. Significant reduction was tested against control. *$P < 0.001$ for uptake by striatum; †$P < 0.001$, ‡$P < 0.01$, and ¶$P < 0.05$ for uptake by cortex; and §$P < 0.05$ for uptake by cerebellum (*t* test, compared with control).

coronal sections of the control rat injected with [^{11}C]KF18446 (Fig. 5A-1 and A-3), a high ^{11}C density was observed in the caudate putamen, nucleus accumbens, and olfactory tubercle; the ^{11}C density was low in the other regions. In the

TABLE 2
Striatal Uptake of 4 ^{11}C-Labeled Tracers Assessed by Ex Vivo ARG in Young Male Wistar Rats at 15 Minutes After Intravenous Injection

Tracer (no. of rats)	Uptake*		Uptake ratio striatum to cortex
	Striatum	Cortex	
[^{11}C]KF18446 (5)	2.19 ± 0.49	0.73 ± 0.20	3.16 ± 0.24
with KF17837 (3)	0.58 ± 0.19	0.43 ± 0.19	1.42 ± 0.17
[^{11}C]KF17837† (4)	0.89 ± 0.18	0.59 ± 0.10	1.51 ± 0.08
with KF17837† (3)	0.61 ± 0.14	0.45 ± 0.11	1.36 ± 0.17
[^{11}C]KF19631 (2)	1.02 ± 0.53	0.67 ± 0.29	1.50 ± 0.06
[^{11}C]CSC (1)	1.64	1.10	1.31

*Uptake in ROI was assessed as the PSL/mm^2/MBq. Injected dose (MBq) was decay corrected to contact time. Mean ± SD.
†Data for [^{11}C]KF17837 were obtained from reference 30.

ARG images of the control rat injected with [^{11}C]KF19631 (Fig. 5B), [^{11}C]CSC (Fig. 5C), and [^{11}C]KF17837 (Fig. 5D), the contrast between the striatum and the other regions was less clear than that for [^{11}C]KF18446. The uptake in the striatum and cortex and the uptake striatum-to-cortex ratios were assessed as the PSL/mm^2/MBq and are summarized in Table 2. Both the striatal uptake of [^{11}C]KF18446 and the

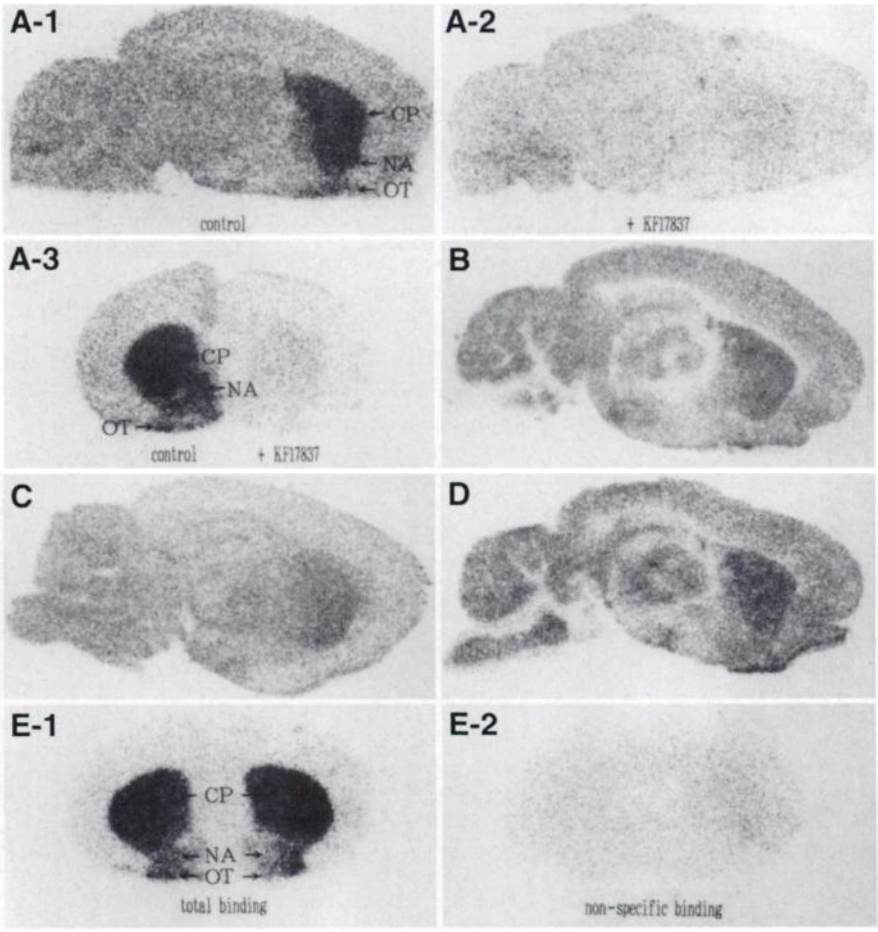

FIGURE 5. Ex vivo (A–D) and in vitro (E) autoradiograms of rat brain section of ^{11}C-labeled tracers. Ex vivo ARG was performed 15 min after intravenous injection of ^{11}C-labeled tracers. (A-1) [^{11}C]KF18446; (A-2) [^{11}C]KF18446 with KF17837 loading; (A-3) [^{11}C]KF18446 (left side) and [^{11}C]KF18446 with KF17837 loading (right side), in which right hemisphere of control and left hemisphere of rat given carrier loading tracer were put side by side for comparative demonstration. Coinjected dose of KF17837 was 700 nmol; (B) [^{11}C]KF19631; (C) [^{11}C]CSC; and (D) [^{11}C]KF17837. (E) In vitro autoradiograms with [^{11}C]KF18446 (E-1) and with [^{11}C]KF18446 and KF18446 loading (E-2). CP = caudate putamen; NA = nucleus accumbens; OT = olfactory tubercle.

TABLE 3
Blocking Effects of Adenosine Antagonists on [^{11}C]KF18446-Binding to the Rat Brain Section Measured by In Vitro Autoradiography

Blocker*	Percentage blockade	
	Striatum	Cortex
KF18446	91.3	54.3
SCH 58261	84.8	27.6
CGS 21680	75.7	25.0

*20 μmol/L. K_i values for the adenosine A_{2a} and A_1 receptors are 5.9 nmol/L and 1600 nmol/L for KF18446; 2.3 nmol/L and 121 nmol/L for SCH 58261; and 4.5 nmol/L and 420 nmol/L for CGS 21680 (*33*).

uptake striatum-to-cortex ratio were approximately twice as large as those of 3 other tracers. The high accumulation of [^{11}C]KF18446 in the striatum was diminished to 26% of the control by coinjection of an excess amount of KF17837 (Fig. 5A-2 and A-3). The uptake level in the cortex was also reduced to 59%.

In Vitro ARG Study of [^{11}C]KF18446 in Rat Brain Section

Figure 5E shows the in vitro autoradiographic images of the coronal brain sections with [^{11}C]KF18446. The total binding of [^{11}C]KF18446 was also concentrated in the caudate putamen, nucleus accumbens, and olfactory tubercle (Fig. 5E-1). The total binding striatum-to-cortex ratio was 8.4 ± 2.2 (n = 3). Table 3 summarizes blocking effects of an excess amount of KF18446 (Fig. 5E-2), SCH 58261, and CGS 21680 on the [^{11}C]KF18446-binding. KF18446 showed the largest blockade (>90%), followed by SCH 58261 and CGS 21680. In the cortex, approximately half of the [^{11}C]KF18446 binding to the cortex was blocked by KF18446, but the blocking effect of SCH 58261 and CGS 21680 was smaller.

PET Study in a Monkey

Figure 6 shows images of the rhesus monkey brain acquired by PET with [^{11}C]KF18446 and T2-weighted MRI of roughly corresponding slices. A high uptake of radioactivity was observed in the striatum. The uptake was also visualized in the cortex, cerebellum, and thalamus. ROIs were placed based on the MRI, and the time–activity curves in the these regions during 60 min are shown in Figure 7. The radioactivity level (SUV) in the striatum was slightly higher than those in other brain regions. The striatal activity level was retained for the initial 20 min and then gradually decreased with time. The uptake ratios of striatum to cortex and striatum to cerebellum gradually increased to approximately 1.5 at 60 min (Table 4). SUVs in plasma were 2.22 at 1 min, 0.91 at 5 min, 0.68 at 15 min, 0.43 at 30 min, and 0.28 at 60 min. Percentages of unchanged [^{11}C]KF18446 in the plasma were >99% at 1 min, 67.2% at 5 min, 57.9% at 15 min, 41.7% at 30 min, and 28.7% at 60 min.

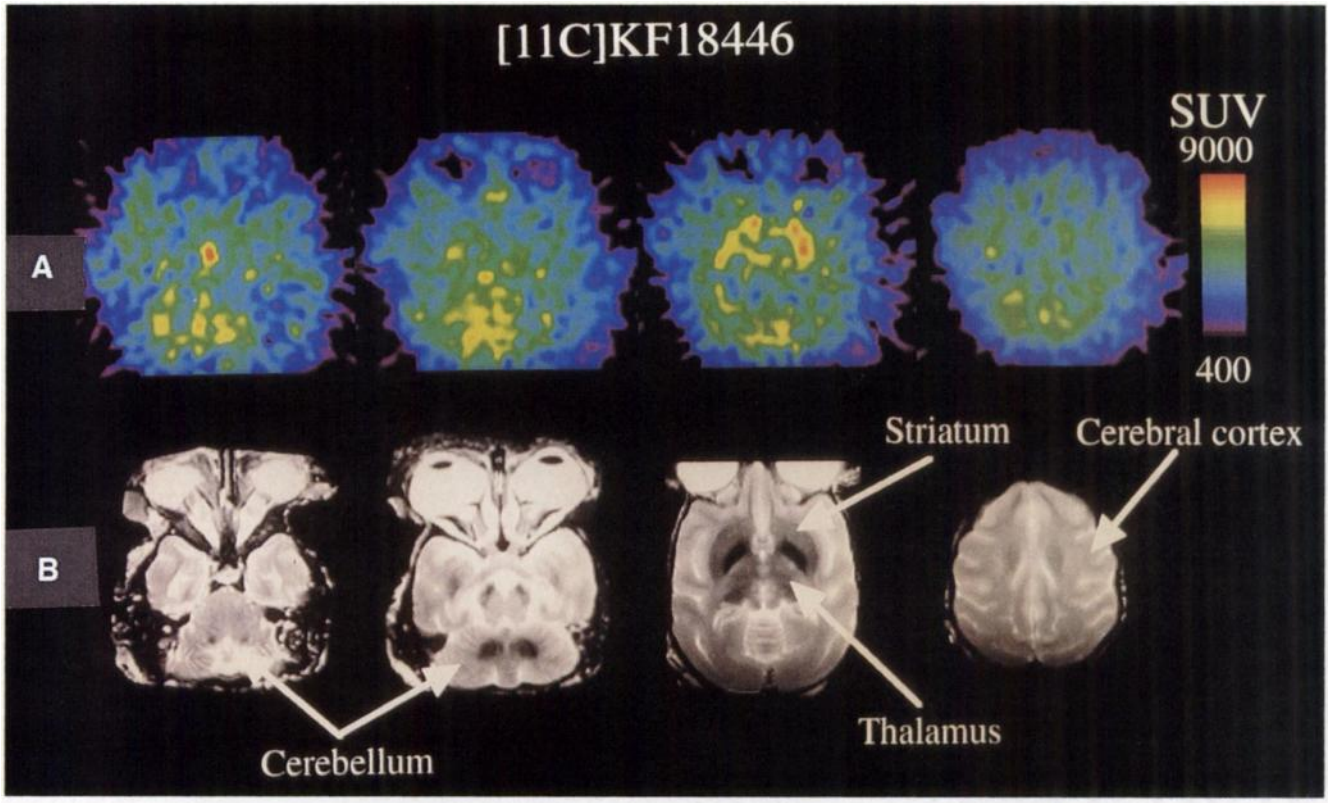

FIGURE 6. Brain PET image of anesthetized monkey scanned with [^{11}C]KF18446. (A) PET images; (B) MR images. PET images were acquired for 50 min starting at 10 min after injection. Injection dose was 102 MBq/2.2 nmol. Values in color scale are SUV × 10^4.

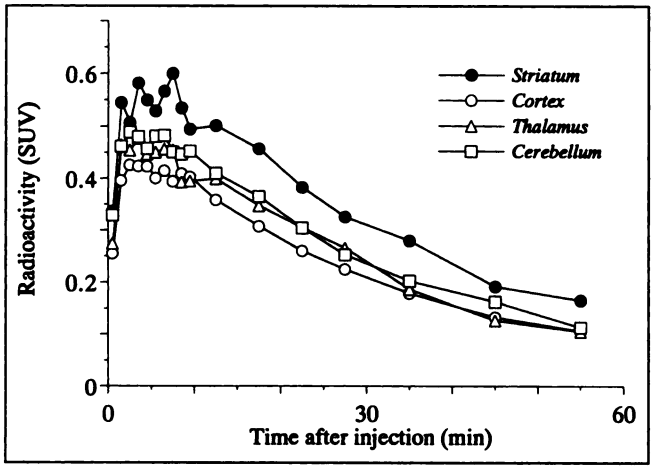

FIGURE 7. Time–activity curves on rhesus monkey brain after intravenous injection of [^{11}C]KF18446.

DISCUSSION

In this study, we compared the potential of 4 ^{11}C-labeled xanthine-type adenosine A_{2a} receptor antagonists as PET ligands for mapping adenosine A_{2a} receptors in the CNS, and have found that [^{11}C]KF18446 is the most suitable tracer.

By the tissue-sampling method in mice and ex vivo ARG in rats, all 4 tracers were taken up by the striatum, which is rich in adenosine A_{2a} receptors, at a higher level than by the other brain regions. This is consistent with the distribution of the adenosine A_{2a} receptors measured by an in vitro binding assay with the brain membrane fraction (*9*) or by in vitro ARG (*10*). Among the 4 tracers, [^{11}C]CSC was rapidly washed out from the brain in vivo (Fig. 2). [^{11}C]KF19631 accumulated in the cortex and cerebellum in the same way as was previously observed for [^{11}C]KF17837 (*30*), whereas [^{11}C]KF18446 gradually decreased in these tissues.

As for the striatal uptake and the uptake ratios of striatum to other regions, [^{11}C]KF18446 may be the most suitable PET ligand among the 4 tracers. The [^{11}C]KF18446 showed higher uptake ratios of striatum to other regions in 3 animal species than did the other 3 compounds (Table 4), which was clearly demonstrated in the ex vivo ARG (Fig. 5). The uptake ratios of striatum to other regions were lower in monkey brain than in rat and mouse brain. This difference is explained mainly by the partial-volume effect based on limited spatial resolution of PET. When the partial-volume effect was simulated mathematically, based on the resolution of PET camera used, and the area of monkey striatum measured by MRI (*37*), the striatal activity was underestimated by about 40% by PET. Thus, the uptake ratio in monkey brain may be compatible with that in rat and mouse brain. In monkey brain, the isoflurane anesthesia may also affect the regional brain uptake of [^{11}C]KF18446. The striatal uptake of [^{11}C]KF18446 was approximately twice as large as that of [^{11}C]KF17837 in mice and rats (Table 4). Although Stone-Elander et al. (*31*) pointed out low penetration of the [^{11}C]KF17837 through the blood–brain barrier in monkeys, the striatal uptake of [^{11}C]KF18446 in a monkey measured by PET (Fig. 6) was approximately 10-fold higher at 5–10 min compared with our previous results with [^{11}C]KF17837 (*30*), and the uptake ratios of striatum to cortex and striatum to cerebellum were slightly improved in the monkey (Table 4). Compared with [^{11}C]KF17837, a slightly lower affinity of [^{11}C]KF18446 (K_i, 5.9 nmol/L for [^{11}C]KF18446 and 1.0 nmol/L for [^{11}C]KF17837) resulted in a gradual decrease in the striatal uptake of the [^{11}C]KF18446.

The in vivo blocking study (Table 1) suggests again the superiority of [^{11}C]KF18446 compared with [^{11}C]KF19631 and [^{11}C]KF17837. Coinjection of KF17837, which has the highest affinity for A_{2a} receptors among the 4 xanthine antagonists examined, reduced the uptake of [^{11}C]KF18446 to 28% of the control in the striatum, whereas the corresponding values were 67% for [^{11}C]KF19631 and 57% for [^{11}C]KF17837.

As for the [^{11}C]KF18446 binding to rat brain, the total binding ratio of striatum to cortex in the in vitro ARG study was approximately threefold as large as that in the ex vivo ARG study, although the ARG was performed at 15 min postinjection, when high uptake ratios of striatum to cortex and striatum to cerebellum were found in mice. The nonspecific binding in the striatum was only 9% in vitro, whereas it was 26% ex vivo. The most probable reason for this discrepancy is the methodological basis. The nonspecifically bound ligand is most likely washed away more efficiently in the in vitro experiments, compared with the slower in vivo clearance. The effect of metabolism of [^{11}C]KF18446 on the nonspecific binding in vivo may be negligible as discussed below.

As for metabolism, [^{11}C]KF18446 was stable to metabolic

TABLE 4
Uptake Ratios of 3 ^{11}C-Labeled Tracers in Mice, Rats, and a Monkey

Tracer	Uptake site	5 min	15 min	30 min	60 min
[^{11}C]KF18446					
Mouse	Striatum/cortex	2.32	2.82	2.85	2.53
	Striatum/cerebellum	2.08	2.71	2.64	2.55
Rat	Striatum/cortex		3.16		
	Striatum/cerebellum		2.67		
Monkey	Striatum/cortex	1.30	1.40	1.47	1.56
	Striatum/cerebellum	1.20	1.22	1.26	1.46
[^{11}C]KF19631					
Mouse	Striatum/cortex	1.03	1.19	1.33	1.57
	Striatum/cerebellum	0.94	0.97	1.03	1.23
Rat	Striatum/cortex		1.50		
	Striatum/cerebellum		1.24		
[^{11}C]KF17837*					
Mouse	Striatum/cortex	1.02	1.37	1.43	2.14
	Striatum/cerebellum	0.90	1.17	1.14	2.03
Rat	Striatum/cortex		1.51		
	Striatum/cerebellum		1.17		
Monkey	Striatum/cortex	1.18	1.31	1.28	1.29
	Striatum/cerebellum	1.05	1.18	1.19	1.27

*Data for [^{11}C]KF17837 were obtained from reference 30.

alteration. Over 80% of the radioactivity in the plasma of mice was detected in the unchanged form for 30 min postinjection, when the analysis was carefully undertaken under dim light to prevent the isomerization of [^{11}C]KF18446. A preliminary metabolite study in monkeys suggested that peripheral degradation of [^{11}C]KF18446 seemed to be faster than in mice. On the other hand, the labeled metabolites were negligible in the brain tissues of mice. This is a striking contrast to the metabolism of the xanthine-type adenosine A_1 ligand [^{11}C]KF15372 and its derivative (*27,28*). They were degraded faster in the plasma than in [^{11}C]KF18446, and their labeled metabolites were also detected in brain tissues.

This study also showed the presence of saturable binding sites for the 3 ^{11}C-labeled KF compounds in the cortex and cerebellum that had been considered to lack A_{2a} receptors (Table 1). For example, coinjection of KF17837 reduced the uptake of [^{11}C]KF18446 to 63% and 62% of the control in the cortex and cerebellum, respectively, and the corresponding figures were 55% and 54% for [^{11}C]KF19631 and 68% and 56% for [^{11}C]KF17837. However, recent in vitro studies also showed that the A_{2a}-like receptors were also found in the hippocampus and cortex (*11–14*). The binding of a standard A_{2a} receptor ligand [^{3}H]CGS 21680 in these tissues may be distinctly different from the classic adenosine A_{2a} receptors present in the striatum and was also different from other defined receptor subtypes.

The reported B_{max} and K_d values are 353 pmol/mg protein and 58 nmol/L in the hippocampus, 264 pmol/mg protein and 58 nmol/L in the cortex, and 419 pmol/mg protein and 17 nmol/L in the striatum (*14*). The cortical binding site of [^{3}H]CGS 21680 was clearly discriminated with another selective adenosine A_{2a} receptor antagonist SCH 58261 (*38*). These findings may explain why the 3 ^{11}C-labeled KF compounds bound to specific binding sites (atypical A_{2a} receptors) in the cortex and cerebellum in this study. Figure 3 indicates that the time courses of the uptake of these compounds in the cortex and cerebellum were qualitatively different from those in the striatum, suggesting that the tracer binding in the cortex and cerebellum may have different kinetics from that in the striatum. PET measurement of monkey brain also showed a comparable tracer uptake in the thalamus, cortex, and cerebellum. The specific binding of [^{3}H]CGS 21680 and [^{3}H]SCH 58261 was also found in certain thalamic nuclei and throughout the cerebral cortex by in vitro ARG of postmortem human brain (*39*).

Currently, a selective A_{2a} receptor agonist [^{3}H]CGS 21680 is widely used as a standard ligand for in vitro studies of adenosine A_{2a} receptors. The characteristics of radiolabeled KF18446 were slightly superior to those of [^{3}H]CGS 21680. In the membrane binding studies, the A_{2a}/A_1 selectivity was 270 for [^{11}C]KF18446 and 94 for [^{3}H]CGS 21680 (*33*). By in vitro ARG, nonspecific binding of [^{11}C]KF18446 in the striatum was 9% of the total binding, whereas the corresponding value for [^{3}H]CGS 21680 was estimated to be 19% (*10*). The total binding ratio of striatum to cortex was 8.4 for [^{11}C]KF18446 and 4.6 for [^{3}H]CGS 21680 (*13*). The present in vitro ARG study (Table 3) shows that the [^{11}C]KF18446-binding to the striatum was competitively reduced by CGS 21680 and another selective adenosine A_{2a} receptor antagonist SCH 58261, whereas the blocking effect was the largest in the self-competition (KF18446 > SCH 58261 > CGS 21680). A similar but smaller blocking effect was also found in the [^{11}C]KF18446-binding in the cortex. These results indicate that the major binding sites of these 4 compounds are typical adenosine A_{2a} receptors in the striatum. The results also provide additional evidence for the presence of unknown specific sites (atypical adenosine A_{2a} receptors) that differ from any of the defined adenosine receptors as discussed previously (*11–14,38*). We performed an in vitro membrane binding assay of KF18446 for several other neuroreceptors: adrenergic α_1, α_2, and β_1; dopamine D_1 and D_2; agonist site of $GABA_A$ and benzodiazepine site of $GABA_A$; histamine H_1 and H_2; nonselective muscarine; nicotinic acetylcholine; and serotonin 5-HT_{1A} and 5-HT_2. The affinity of KF18446 could not be detected for any of these receptors (<10 μmol/L of K_d values).

An interesting finding is that a nonxanthine-type adenosine A_{2a} receptor antagonist SCH 58261 significantly reduced the striatal uptake of only [^{11}C]KF18446 in the in vivo experiment (Table 1). Although the K_i value of SCH 58261 for the A_{2a} receptors (*34*) is the same magnitude of order as those of the 3 KF compounds in the membrane binding assay using [^{3}H]CGS 21680 as a radioligand, the blocking effect of SCH 58261 was smaller than that of the 3 KF compounds. The 3 xanthine-type KF compounds and SCH 58261 may recognize in vivo different binding sites besides the typical A_{2a} receptors as discussed earlier. We also reported a similar phenomenon supporting this speculation. In a previous study, the striatal uptake of [^{11}C]KF17837 was not blocked by SCH 58261 or by another nonxanthine antagonist, ZM 241385 (*30*). Among the peripheral organs, [^{11}C]KF17837 was taken up by the heart in mice (*29*) and in rabbits (*40*), which suggests its affinity for the myocardial adenosine A_{2a} receptors. The PET study in rabbits showed that the blocking effect of SCH 58261 and ZM 241385 on the myocardial uptake of [^{11}C]KF17837 was smaller than that of CSC (*40*). The different blocking effects between xanthine and nonxanthine adenosine A_{2a} antagonists on the myocardial uptake of [^{11}C]KF19631 in mice were also found (unpublished data). Blockade of the striatal uptake of [^{11}C]KF18446 by SCH 58261 may reflect that the affinity of KF18446 for adenosine A_{2a} receptors is slightly lower than that of KF17837 and KF19631, and that KF18446 may have a property analogous to SCH 58261 for the A_{2a} receptors. The binding properties of various A_{2a} receptor antagonists and agonists is now under investigation in vitro and in vivo.

CONCLUSION

The regional brain distribution and blocking studies in mice and the ex vivo ARG with blocking studies in rats have shown that all 4 ^{11}C-labeled xanthine-type antagonists demonstrate specific accumulation in the striatum, in which adenosine A_{2a} receptors are exclusively localized. However, the presence of atypical binding sites for these xanthine compounds was suggested in other brain regions, such as the

cerebral cortex and cerebellum. As for the selectivity for the striatum, [^{11}C]KF18446 is much superior to [^{11}C]KF19631 or [^{11}C]KF17837. As demonstrated in a PET study of a rhesus monkey, [^{11}C]KF18446 has a potential as a PET tracer for mapping adenosine A_{2a} receptors in the brain.

ACKNOWLEDGMENTS

This study was presented in part at the 12th International Symposium on Radiopharmaceutical Chemistry, June 15–19, 1997, in Uppsala, Sweden. This work was supported by a Grant in Aid for Scientific Research (08557045) from the Ministry of Education, Science, Sports, and Culture, Japan. The authors thank Drs. M. Ito and S. Shibabe for the advice and discussion in ARG studies, and the Radioisotope School Nuclear Education Center, the Japan Atomic Energy Research Institute (Tokyo, Japan), where analysis of the ARG was performed. The authors also thank S. Ishii and M. Toyoda for their assistance in radiosynthesis; Dr. H. Nonaka and T. Itou for their help in the biological study; Dr. S. Shumiya, Dr. H. Toyama, K. Oda, and M. Ando for their assistance in the PET study; and Dr. T. Nagaoka for his technical support with MRI.

REFERENCES

1. Fredholm BB, Abbracchio MP, Burnstock G, et al. Nomenclature and classification of purinoceptors. *Pharmacol Rev.* 1994;46:143–156.
2. Palmer TM, Stiles GL. Adenosine receptors. *Neuropharmacology.* 1995;34:683–694.
3. Ongini E, Fredholm BB. Pharmacology of adenosine A_{2A} receptors. *Trends Pharmacol Sci.* 1996;17:364–372.
4. Lewis ME, Patel J, Moon Edley S, Marangos PJ. Autoradiographic visualization of rat brain adenosine receptors using N^6-cyclohexyl[^{3}H]adenosine. *Eur J Pharmacol.* 1981;73:109–110.
5. Goodman RR, Snyder SH. Autoradiographic localization of adenosine receptors in rat brain using [^{3}H]cyclohexyladenosine. *J Neurosci.* 1982;2:1230–1241.
6. Fastbom J, Pazos A, Palacios JM. The distribution of adenosine A1 receptors and 5′-nucleotidase in the brain of some commonly used experimental animals. *Neuroscience.* 1987;22:813–826.
7. Fastbom J, Pazos A, Probst A, Palacios JM. Adenosine A1 receptors in the human brain: a quantitative autoradiographic study. *Neuroscience.* 1987;22:827–839.
8. Mally J, Stone TW. Potential role of adenosine antagonist therapy in pathological tremor disorders. *Pharmacol Ther.* 1996;72:243–250.
9. Bruns RF, Lu GH, Pugsley TA. Characterization of A_2 adenosine receptor labeled with [^{3}H]NECA in rat striatal membranes. *Mol Pharmacol.* 1986;29:331–346.
10. Parkinson FE, Fredholm BB. Autoradiographic evidence for G-protein coupled A_2-receptors in rat neostriatum using [^{3}H]-CGS21680 as a ligand. *Naunyn Schmied Arch Pharmacol.* 1990;342:85–89.
11. Cunha RA, Johansson B, van der Ploeg I, Sebastião AM, Ribeiro JA, Fredholm BB. Evidence for functionally important adenosine A_{2A} receptors in the rat hippocampus. *Brain Res.* 1994;649:208–216.
12. Kirk IP, Richardson PJ. Further characterization of adenosine A_{2a} receptor-mediated modulation of [^{3}H]CGS 21680 binding sites in the rat striatum and cortex. *Br J Pharmacol.* 1995;114:537–543.
13. Johansson B, Georgiev V, Parkinson FE, Fredholm BB. The binding of the adenosine A_2 selective agonist [^{3}H]CGS 21680 to rat cortex differs from its binding to rat striatum. *Eur J Pharmacol.* 1993;247:103–110.
14. Cunha RA, Johansson B, Constantino MD, Sebastião AM, Fredholm BB. Evidence for high-affinity binding sites for the adenosine A_{2A} receptor agonist [^{3}H]CGS 21680 in the rat hippocampus and cerebral cortex that are different from striatal A_{2A} receptors. *Naunyn Schmied Arch Pharmacol.* 1996;353:261–271.
15. Schiffmann SN, Libert F, Vassart G, Vanderhaeghen JJ. Distribution of adenosine A_2 receptor mRNA in the human brain. *Neurosci Lett.* 1991;130:177–181.
16. Pollack AE, Harrison MB, Wooten GF, Fink JS. Differential localization of A2a adenosine receptor mRNA with D1 and D2 dopamine receptor mRNA in striatal output pathways following a selective lesion of striatonigral neurons. *Brain Res.* 1993;631:161–166.
17. Martinez-Mir MI, Probst A, Palacios JM. Adenosine A2 receptors: selective localization in the human basal ganglia and alterations with disease. *Neuroscience.* 1991;42:697–706.
18. Ferré S, von Euler G, Johansson B, Fredholm BB, Fuxe K. Stimulation of high-affinity adenosine A_2 receptors decreases the affinity of dopamine D_2 receptors in rat striatal membranes. *Proc Natl Acad Sci USA.* 1991;88:7238–7241.
19. Vellucci SV, Sirinathsinghji DJS, Richardson PJ. Adenosine A_2 receptor regulation of apomorphine-induced turning in rats with unilateral striatal dopamine denervation. *Psychopharmacology.* 1993;111:383–388.
20. Parsons B, Togasaki DM, Kassir S, Przedborski S. Neuroleptic up-regulate adenosine A_{2a} receptors in rat striatum: implication for the mechanism and the treatment of tardive dyskinesia. *J Neurochem.* 1995;65:2057–2064.
21. Ferré S, Fredholm BB, Morelli M, Popoli P, Fuxe K. Adenosine-dopamine receptor-receptor interactions as an integrative mechanism in the basal ganglia. *Trends Neurosci.* 1997;20:482–487.
22. Ferré S. Adenosine-dopamine interactions in the ventral striatum: implications for the treatment of schizophrenia. *Psychopharmacology.* 1997;133:107–120.
23. Guieu R, Couraud F, Pouget J, Sampieri F, Bechis G, Rochat H. Adenosine and the nervous system: clinical implications. *Clin Neuropharmacol.* 1996;19:459–474.
24. Jacobson KA, von Lubitz DKJE, Daly JW, Fredholm BB. Adenosine receptor ligands: differences with acute versus chronic treatment. *Trends Pharmacol Sci.* 1996;17:108–113.
25. Baldessarini RJ. Drugs and the treatment of psychiatric disorders. In Goodman GA, Rall TW, Nies AS, Taylor P, eds. *Pharmacological Bases of Therapeutics.* New York, NY: Pergamon; 1990:383–435.
26. Ferré S, O'Connor WT, Snaprud P, Ungerstedt U, Fuxe K. Antagonistic interaction between adenosine A_{2A} receptors and dopamine D_2 receptors in the ventral striopallidal system. Implications for the treatment of schizophrenia. *Neuroscience.* 1994;63:765–773.
27. Furuta R, Ishiwata K, Kiyosawa M, et al. Carbon-11 labeled KF15372:a potential central nervous system adenosine A_1 receptor ligand. *J Nucl Med.* 1996;37:1203–1207.
28. Noguchi J, Ishiwata K, Furuta R, et al. Evaluation of carbon-11 labeled KF15372 and its ethyl and methyl derivatives as a potential CNS adenosine A_1 receptor ligand. *Nucl Med Biol.* 1997;24:53–59.
29. Ishiwata K, Noguchi N, Toyama H, et al. Synthesis and preliminary evaluation of [^{11}C]KF17837, a selective adenosine A_{2A} antagonist. *Appl Radiat Isot.* 1996;47:507–511.
30. Noguchi J, Ishiwata K, Wakabayashi S, et al. Evaluation of carbon-11 labeled KF17837: a potential CNS adenosine A_{2a} receptor ligand. *J Nucl Med.* 1998;39:498–503.
31. Stone-Elander S, Thorell J-O, Eriksson L, Fredholm BB, Ingvar M. *In vivo* biodistribution of [*N*-^{11}C-methyl]KF 17837 using 3-D-PET: evaluation as a ligand for the study of adenosine A_{2A} receptors. *Nucl Med Biol.* 1997;24:187–191.
32. Jacobson KA, Gallo-Rodriguez C, Melman N, et al. Structure-activity relationships of 8-styrylxanthines as A_2-selective adenosine antagonists. *J Med Chem.* 1993;36:1333–1342.
33. Nonaka H, Ichimura M, Takeda M, et al. KF17837 ((*E*)-8-(3,4-dimethoxystyryl)-1,3-dipropyl-7-methylxanthine) a potent and selective adenosine A_2 receptor antagonist. *Eur J Pharmcol.* 1994;267:335–341.
34. Zocchi C, Ongini E, Ferrara S, Baraldi PG, Dionisotti S. Binding of the radioligand [^{3}H]-SCH 58261, a new non-xanthine A_{2A} adenosine receptor antagonist, to rat striatal membranes. *Br J Pharmacol.* 1996;117:1381–1386.
35. Suzuki F, Shimada J, Mizumoto H, et al. Adenosine A_1 antagonists. 2. Structure-activity relationships on diuretic activities and protective effects against acute renal failure. *J Med Chem.* 1992;35:3066–3075.
36. Przedborski S, Levivier M, Jiang H, et al. Dose-dependent lesions of the dopaminergic nigrostriatal pathway induced by intrastriatal injection of 6-hydroxydopamine. *Neuroscience.* 1995;67:631–647.
37. Uemura K, Toyama H, Ikoma Y, et al. Effects of heterogeneity and resolution on rate constant estimation in compartment model analysis of FDG PET [abstract]. *Eur J Nucl Med.* 1998;25:1149.
38. Lindström K, Ongini E, Fredholm BB. The selective adenosine A_{2A} receptor antagonist SCH 58261 discriminates between two different binding sites for [^{3}H]-CGS 21680 in the rat brain. *Naunyn Schmied Arch Pharmacol.* 1996;354:539–541.
39. Svenningsson P, Hall H, Sedvall G, Fredholm BB. Distribution of adenosine receptors in the postmortem human brain: an extended autoradiographic study. *Synapse.* 1997;27:322–335.
40. Ishiwata K, Sakiyama Y, Sakiyama T, et al. Myocardial adenosine A_{2a} receptor imaging of rabbit by PET with carbon-11-KF17837. *Ann Nucl Med.* 1997;11:219–225.